Influence of PVP content on degradation of PES/PVP membranes: insights from characterization of membranes with controlled composition

Yamina Kourde-Hanafi[1,2], Patrick Loulergue[1*], Anthony Szymczyk[1], Bart Van der Bruggen[3], Manfred Nachtnebel[4], Murielle Rabiller-Baudry[1], Jean-Luc Audic[1] , Peter Pölt[4,5], Kamel Baddari[2]

[1]Université de Rennes 1, Université Bretagne-Loire, Institut des Sciences Chimiques de Rennes (UMR CNRS 6226), 263 Avenue du Général Leclerc, CS 74205, 35042 Rennes, France

[2]Unité de Recherche Matériaux Procédés et Environnement, Université M'hamed Bougara, Boumerdes, Algeria

[3]Department of Chemical Engineering, KU Leuven, Celestijnenlaan 200F, B-3001 Heverlee, Belgium

[4]Institute for Electron Microscopy and Nanoanalysis, NAWI Graz, Graz University of Technology, Steyrerg. 17, 8010 Graz, Austria

[5]Graz Centre for Electron Microscopy, Steyrerg. 17, 8010 Graz, Austria

* corresponding author : patrick.loulergue.1@univ-rennes1.fr

Univ. Rennes 1 – ISCR, Bat 10A, 263 Avenue du Général Leclerc, CS 74205, 35042 Rennes, France

Abstract: Sodium hypochlorite is widely used to clean/sanitize PES/PVP membranes. However, this strong oxidant is responsible for accelerated polymer ageing, thus impairing PES/PVP membrane lifespan. This work aimed at getting a better understanding of the role of PVP in the degradation of PES/PVP membranes. As the precise chemical composition of commercial membranes is most often unknown, PES/PVP membranes with various PVP to PES ratios (from 0 to 44 wt %) were synthesized and aged dynamically by filtering sodium hypochlorite solutions. PVP oxidization and partial disappearance from the membrane matrix was observed whatever the membrane composition. Moreover, PES-chain scissions were put in evidence even for pure PES membranes, thus highlighting that PES degradation was not systematically related to the presence of PVP. Conversely, PES hydroxylation was observed only for membranes containing PVP, the hydroxylation rate being dependent on the PVP content. Interestingly, the occurrence of PES-chain scissions impacted the membrane filtration performance while no correlation was found between the PES hydroxylation rate and the filtration performance.

Keywords: membrane ageing; PES/PVP membrane; PVP content; sodium hypochlorite

Highlights:

- PES/PVP polymeric membranes ageing due to dynamical NaOCl exposure
- Impact of PVP content on PES membrane degradation mechanisms
- PVP leakage and PES chain scission whatever the membrane composition
- PES hydroxylation depends on PVP content
- No impact of PES hydroxylation on filtration performance

Introduction

Membrane filtration processes are now widely used in environmental applications (water and wastewater treatment), and in a number of industries including agri-food and biotechnology industries. The relatively low manufacturing cost of polymeric membranes together with the easy processing of large-area membranes have led to a dominant position of polymeric membranes worldwide. Among the many polymers used as membrane materials, polyethersulfone (PES, see figure 1) is widely used to synthesize microfiltration and ultrafiltration membranes as PES has both excellent chemical and thermal resistances over a wide range of pH (from 1 to 13) [1–3]. However, PES is relatively hydrophobic and therefore additives such as polyvinylpyrrolidone (PVP, see figure 1) are usually blended with PES (without covalent bounds between the two polymers), in order to increase the membrane hydrophilicity. PVP also plays the role of pore former during the membrane synthesis by phase inversion. Depending on the polymer properties and the additive-to-polymer ratio it is therefore possible to prepare membranes with different morphologies (pore structure) and hydrophilicities, and then with different performance in terms of permeability, rejection or fouling resistance [4–7].

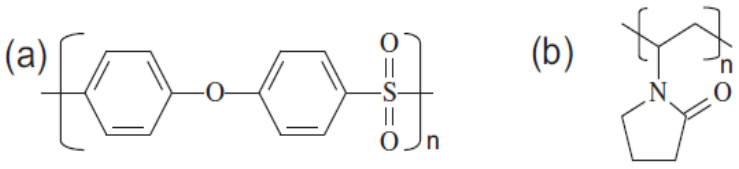

Figure 1: Chemical structures of Polyethersulfone (a) and Polyvinylpyrrolidone (b).

One of the major problems associated with the use of such membranes, especially when filtering organic species, is fouling, which impairs filtration performance. Furthermore, non-negligible irreversible fouling (i.e. the part of fouling that cannot be removed by a simple water rinsing) is often observed. At the industrial scale, cleaning-in-place/disinfection steps using various chemicals in cascade are then performed periodically so as to mitigate fouling and restore membrane performance. Sodium hypochlorite is one of the most widely-used disinfecting/cleaning agents owing to its high efficiency and low cost [8–10]. However, it is well known that sodium hypochlorite has a strong impact on membranes properties such as structure [2,11,12], surface charge [2,13,14] and chemical composition [3,10,13,15], which directly impacts their filtration performance and their mechanical strength as well [3,15,16]. Membrane properties modifications result from chemical reactions between the membrane constituents and the different forms of chlorine in sodium hypochlorite solutions (mainly HClO and ClO^-) as well as hydroxyl radicals (OH°) produced by the reaction between HClO and ClO^- [17,18]).

For instance, PVP is easily oxidized when brought into contact with sodium hypochlorite due to the presence of ClO^- [1,14] or OH° [14,19]. In more drastic ageing conditions dislodgement of PVP from the membrane matrix has even been reported [3,10,13,15,20].

Regarding PES, two different degradation mechanisms by sodium hypochlorite have been reported. Several studies pointed out the occurrence of a PES-chain scission mechanism [2,3,10,13,14,21,22]. For PES (MW = 30,000 g mol^{-1}) dense films containing small amounts of polyetherethersulfone (PEES), PES-chain scissions were observed after long term ageing (8 months) in 28,500 ppm total free chlorine (TFC) NaOCl solutions at pH 9 and 12 [23,24]. The possible role of PEES was not discussed in these works but it was found that the polymer

films degradation was substantially accelerated by the addition of PVP (5 wt %). Recently, Hanafi et al [14] showed that both HClO and OH° were responsible for PES-chain scissions in PES/PVP porous membranes.

The hydroxylation of PES aromatic rings was also reported [13,14,19] and was attributed to a radical attack by OH°. Prulho [19] and co-workers observed that this phenomenon occurred only in the presence of PVP since pure PES films prepared from PES (MW= 37,000 g mol^{-1}) were not degraded after 176 h in 4,000 ppm TFC sodium hypochlorite solutions at pH 8 and pH 12, while PES oxidization was observed for PES/PVP blends (50/50 wt %) just after a few-hour ageing. These authors suggested that by-products might be formed during PVP degradation and might further attack PES. However, although they were able to highlight the formation of phenol groups (i.e. the attachment of hydroxyl groups on the PES aromatic rings) thanks to ATR-FTIR analyses run in a particularly accurate way, no experimental proof was provided for the attachment of other organic functional groups on the PES backbone [19]. Based on the PVP structure, radical by-products that might be formed as a result of PVP degradation would be quite highly substituted and relatively stable, and then less reactive than OH°.

Finally, the presence of chlorine on PES/PVP membranes aged by NaOCl was also evidenced from SEM-EDX analyses. Since no cation was detected along with chlorine it was concluded that chlorine was most probably covalently bonded to the membrane backbone and not adsorbed in a salt form (i.e. Cl^- together with a charge-balancing cation) [10,23]. Such an observation was in good agreement with further investigations carried out by Hanafi et al who used XPS to show the existence of C-Cl bonds on aged membranes while no chlorine was observed on pristine membrane surfaces [14].

These results indicate that the mechanisms leading to PES membrane degradation by sodium hypochlorite remain unclear. In particular the role of PVP, which is the most common additive used in the synthesis of PES membranes, still has to be investigated.

One of the major bottlenecks when studying membrane degradation mechanisms is that the exact chemical composition of commercial membranes is generally unknown, as both the nature and the amount of additives are generally not provided by membrane manufacturers.

In order to get a better understanding of the role played by PVP in PES/PVP membrane ageing, lab-made PES/PVP porous membranes were considered in the present work. Pure PES membranes and membranes with different PES to PVP ratio (from 4 to 44 wt % of PVP) were synthesized and chemically aged by 200 ppm TFC hypochlorite solutions at pH 8 under dynamic conditions (filtration during 20 h at room temperature). ATR-FTIR spectroscopy and streaming current measurements were combined in order to evaluate the implication of the PVP in the different PES degradation mechanisms (PES-chain scission and PES hydroxylation) and the impact of each mechanism on the filtration performance (hydraulic permeability and neutral solute rejection).

2. Materials and methods

2.1. Chemicals

Polyethersulfone (PES, Veradel P 3100, MW = 35,000 g mol^{-1}) supplied by Solvay Advanced Polymer (Belgium) and N-Methyl-2-pyrrolidone (NMP, purity of 99.5 % purchased from

Sigma-Aldrich, Germany) were used to prepare casting solutions for membrane preparation. Polyvinylpyrrolidone (MW = 40,000 g mol^{-1}) was used as an hydrophilic additive and pore former agent.

Bleach solution (NaOCl, La Croix, France – TFC: 96,000 ppm) was diluted to prepare the hypochlorite solutions used for ageing experiments. The solution pH was adjusted with 0.1 mol L^{-1} HCl solutions of analytical grade (Fischer Scientific).

Polyethylene glycols (PEG; Fluka) with different molecular weights (4,000; 10,000; 20,000 and 35,000 g mol^{-1}) were used for rejection tests.

All electrokinetic measurements were conducted with 0.001 mol L^{-1} KCl background solutions, the pH of which was adjusted with 0.1 mol L^{-1} HCl and KOH solutions (Fischer Scientific, analytical grade).

All solutions were prepared using deionized water (resistivity: 18 MΩ cm).

2.2. Membrane synthesis

Membranes with different compositions (Table 1) were synthesized by the non-solvent induced phase separation method. The casting solutions were prepared by incorporating the required amount of PES, PVP and NMP in a round bottom flask under continuous stirring (600 rpm) at room temperature (23°C) for at least 24 h, until the polymer was completely dissolved. Subsequently, air bubbles that might be trapped in the polymer solution were removed by a vacuum pump (15 min at 40°C). The resulting homogeneous solutions were then cast uniformly using an automatic filmograph (K4340 automatic film applicator, Elcometer) with a 250 µm casting knife (casting speed 20 mm s^{-1}) onto a non-woven

polypropylene/polyethylene Viledon FO 2471 support (Freudenberg, Germany) tightly attached onto a glass plate. Casting was performed at 20°C and at a constant relative humidity of 20 %. After casting the glass plate was immediately immersed into a water bath at 23°C to allow polymer coagulation. After 1 h, the resulting membranes were repeatedly washed with distilled water to remove the remaining solvent and were then stored in ultrapure water before use.

Table 1: Casting solution composition

PVP/PES ratio (wt %)	NMP (g)	PES (g)	PVP (g)
0	75	25	0
4	75	25	1
16	75	25	4
32	75	25	8
44	75	25	11

2.3. Ageing procedure

Dynamical ageing experiments were performed by filtering 200 ppm TFC NaOCl solutions at pH 8 and room temperature. These ageing conditions were selected as 200 ppm is a fairly representative concentration of on-site operations and pH 8 is known to have the most drastic effect on PES/PVP membranes [3,14]. Indeed, at pH 8 both HClO and ClO^- species

coexist (HClO representing about 25 % of the TFC against 75 % for ClO^-) and this pH is favorable to produce the maximum amount of free radicals [17]. The ageing solution was filtered for 20 h, the corresponding chlorine dose (concentration x contact time) being 167 ppm day.

The crossflow filtration set-up used to perform dynamical ageing included a 10 L thermally controlled feed tank (25 ± 2 °C) and a plate and frame module (Ray-Flow X100, Novasep-Process, France) with an effective membrane area of about 127 cm^2. After membrane compaction at 2.5 bar (until a constant permeation flux was reached) the bleach solution was filtered at a constant transmembrane pressure (TMP) of 1 bar and a constant cross-flow velocity of 0.26 ± 0.01 m s^{-1} for 20 h. No spacer was added.

2.4. Membrane characterization

Prior to characterization, membrane samples were rinsed thoroughly with deionized water, sonicated twice (2 x 2 min) and then dipped in deionized water for approximately 24 hours in order to remove all traces of bleach solution or possible soluble polymer degradation products.

2.4.1. Filtration performance

The pure water permeability of pristine and aged membranes was measured using the same set-up as for dynamical membrane ageing.

The pure water permeate flux (J_W) of the pristine and aged membranes was measured at different TMP ranging from 0.5 to 2.5 bar so as to determine the pure water permeability

(L_p) from the slope of the plot J_w vs. TMP according to Darcy's law (see example of raw data in the supporting information S1):

$$J_W = L_P \times TMP \quad (1)$$

PEG rejection by the pristine and aged membranes was also studied. A membrane sample was cut and inserted in an Amicon 8050 cell (effective membrane surface area: 13.4 cm^2) connected to a pressurized five-liter vessel containing the feed solution (PEG concentration: 1.0 g L^{-1}). Rejection experiments were carried out in dead-end mode at a TMP of 1 bar. Once a steady-state permeation was reached (it took about 1 hour), both permeate and retentate samples were collected for analysis. PEG concentrations were determined by total organic carbon analysis (TOC-$V_{CPH/CPN}$ Total Organic Analyzer, Shimadzu, Japan). The accuracy on total organic carbon measurement was better than 5 %. PEG rejections (R_{PEG}) were determined from the following equation:

$$R_{PEG} = 100\left(1 - \frac{C_P}{C_f}\right) \quad (2)$$

where C_P is the PEG concentration in the permeate and C_f is the PEG concentration in the feed solution.

2.4.2. Streaming current measurements

A SurPass electrokinetic analyzer (Anton Paar Gmbh, Graz, Austria) equipped with an adjustable-gap cell was used to measure tangential streaming current. Membrane samples (length 2 cm and width 1 cm) were adjusted to the sample holder dimensions and fixed using

214 double-sided adhesive tape. The distance between the membrane samples was set to
215 100 ± 2 µm.

216 Prior to the first measurement, the electrolyte solution was circulated through the channel
217 formed by the membrane samples for at least 2 hours in order to equilibrate the membrane
218 samples with the background solution.

219 The streaming current was measured and recorded for increasing pressure differences up to
220 300 mbar, the flow direction being changed periodically. All experiments were performed at
221 room temperature (20 ± 2 °C) under a controlled atmosphere (nitrogen gas) in order to allow
222 accurate measurements at alkaline pHs (see [25]).

223

224 2.4.3. Fourier Transform Infrared spectroscopy (FTIR)

225 Two different FTIR (Fourier transform infrared) spectroscopy techniques were used to
226 characterize the pristine and aged membranes. Attenuated total reflectance mode (ATR-
227 FTIR) was used to evaluate the chemical modifications undergone by the different
228 membranes exposed to hypochlorite solutions while micro – (transmission) FTIR
229 spectroscopy was used to map the PVP content through the membrane thickness.

230

231 2.4.3.1 ATR-FTIR spectroscopy

232 After careful dynamical vacuum drying (two days) the top surface of membrane samples was
233 characterized using a FT/IR-4100 Fourier Transform Infrared Spectrometer (Jasco) equipped
234 with a ZnSe crystal ATR element (single reflection; incidence angle: 45°). Spectra were

collected from 600 to 3700 cm^{-1} at 2 cm^{-1} resolution and each spectrum was averaged from 128 scans after background recording performed at ambient air.

2.4.3.2 Micro – FTIR spectroscopy

Micro – FTIR spectroscopy allows to map the distribution of the various components of a composite polymer-based membrane across its cross-section [20]. It was used in the present work to map the distribution of both the PES and the PVP through the membrane thickness. To achieve a cross-section mapping using ATR-FTIR, a crystal with a variable incidence angle is needed (as this latter imposes the penetration depth of the incident IR beam in the sample). Nevertheless the porous and composite features of PES/PVP membranes induced some difficulties in the validation of the exact penetration depth. Moreover, the pressure exerted on the flat sample both by the pressure clamp and the ATR crystal can caused geometrical distortions of the samples and thus of the resulting maps. To overcome this issue, suitable thin specimen slices were prepared to examine them in the transmission mode. The samples were firstly embedded in resin to stabilize them and prevent distortion during the slicing process. From all resins tested EpoHeat® (Buehler, Lake Buff, USA) turned out to be the most suitable for embedding the samples, because it was the one with the fewest IR bands overlapping with those of PES and PVP. Thin slices (20 µm), required in transmission mode, were then obtained by applying microtomy over the cross-section of the composite flat membranes.

A Hyperion 3000 FT-IR microscope with a Tensor 27 spectrometer (Bruker, Billerica, USA) was used for recording the mappings. To get the PES distribution, the respective IR band was integrated in the wavenumber range of 1560 cm^{-1} to 1597 cm^{-1}, the assignment of which

corresponds to C=C ring vibration, that for the PVP distribution in the range of 1635 cm^{-1} to 1695 cm^{-1}, the assignment of which corresponds to C=O bound. Because of the inhomogeneous pore-size distribution over the membrane cross-section the material content per volume unit and thus the IR intensity changed. To properly adjust for these intensity changes resulting from the membrane porosity, the PVP/PES distribution was calculated. Occasionally small inclusions in the resin showed IR bands in the same wavenumber region as PVP. By subsequently dividing through a PES concentration close to zero these regions can have very high intensities in the PVP/PES maps. Nevertheless, this method enables at least a qualitative comparison of the distribution of the membrane components of both the pristine membranes and membranes after a chemical treatment.

2.4.4. Scanning Electron Microscopy (SEM)

The membranes were embedded in resin to stabilize them. Subsequently cross sections of the samples were prepared by use of a microtome. Image recording (secondary electrons) was carried out with a scanning electron microscope Zeiss Ultra 55. To avoid charging of the samples, they were coated with a thin (a few nm) gold/palladium layer. To minimize the penetration depth of the electrons in the material and that way also the information depth, an electron energy of 3 keV was chosen. Thus only the topmost pores should be imaged and distortion of pore sizes and shapes be avoided.

3. Results and discussion

3.1 Membrane filtration performance

The pure water permeability of membranes containing different amounts of PVP was determined before and after ageing (Figure 2).

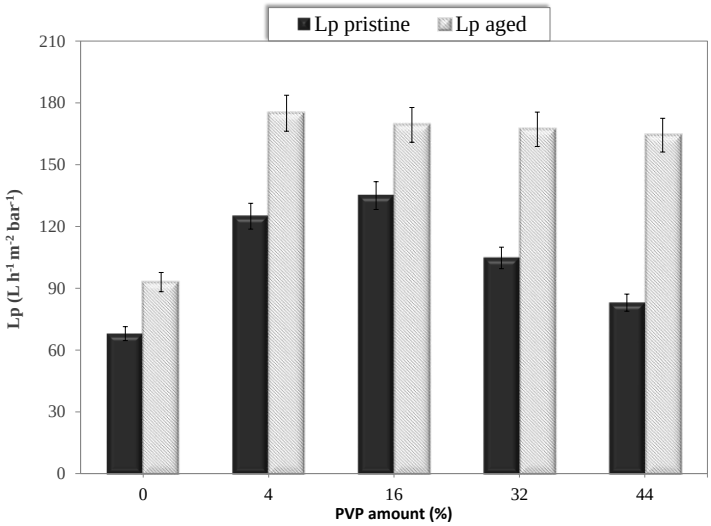

Figure 2: Pure water permeability of pristine and aged membranes with different PVP amounts (0 - 44 wt %).

A strong impact of PVP on membrane permeability was observed. The pure PES membrane had the lowest permeability (around 70 L h^{-1} m^{-2} bar^{-1}) while the most permeable membrane was the one synthesized with 16 % of PVP (135 L h^{-1} m^{-2} bar^{-1}). Despite its hydrophilic nature it was observed that higher PVP concentrations in the casting solution led to a decrease in the membrane permeability. In other words, the permeability did not exhibit a monotonous trend with the amount of PVP. This can be explained by the dual role of PVP, i.e. (i) making the membrane more hydrophilic and (ii) acting as a pore former agent that can either increase or decrease the pore size depending on its concentration in the casting solution. This observation is in line with previous studies and has been explained by the differences in the membrane structure according to the amount of PVP [6,26].

Furthermore, membrane ageing led to an increase in pure water permeability whatever the membrane composition. The pure-PES membrane permeability increased to more than 90 L h^{-1} m^{-2} bar^{-1}. Interestingly, the pure water permeability of aged membranes containing PVP

298 was found to be almost constant and close to 170 L h^{-1} m^{-2} bar^{-1} whatever the PVP amount
299 (in the casting solution).

300 PEG rejections by the pristine and dynamically aged membranes are shown in figure 3.
301 Pristine membrane rejections were very high (> 93 %) for all PEGs (with molecular weights
302 from 4,000 to 35,000 g mol^{-1}) regardless of the PVP content (up to 44 %). Therefore, it can be
303 concluded that the presence of PVP in the membrane body had no significant impact on the
304 membrane rejection performance. After exposure to sodium hypochlorite, lower PEG
305 rejections were observed. A rather high rejection, between 80 and 90 %, was obtained for
306 the PEG with the highest molecular weight (35,000 g mol^{-1}) but a dramatic decrease was
307 observed for the smallest PEG (4,000 g mol^{-1}) with rejection rates between 30 and 60 %. It is
308 worth noting that no correlation was observed between the initial amount of PVP in the
309 membranes and the lowering of aged-membrane rejections.

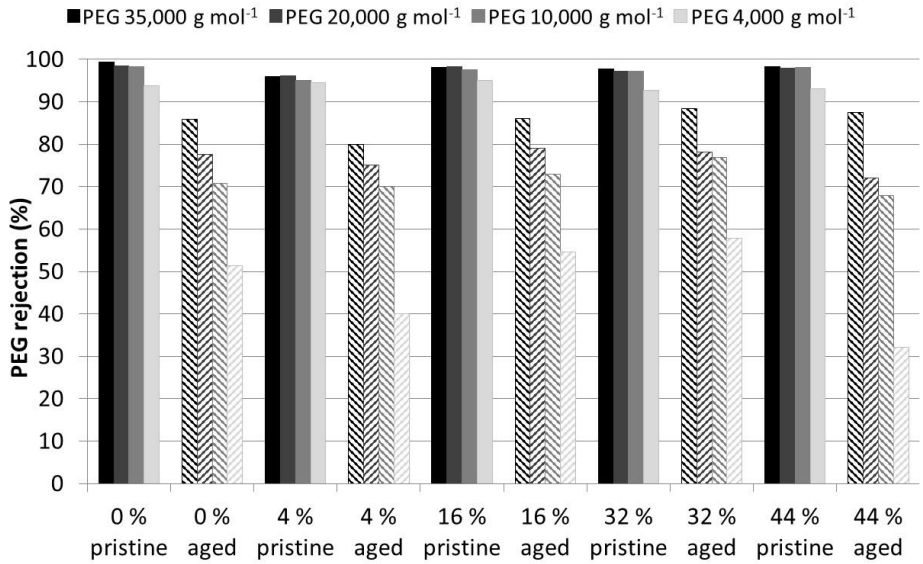

310

311 **Figure 3:** Rejection of PEGs with different molecular weights (4,000; 10,000; 20,000 and
312 35,000 g mol^{-1}) by the pristine and aged membranes synthesized with different PVP amounts
313 (0 - 44 %) (greyscale: pristine membranes, hatched marks: aged membranes).

Since modifications of the membrane performance after ageing were observed for all membrane compositions, even for pure PES, it can be concluded that these changes were related, at least partly, to the modification of the PES backbone itself. Interestingly, the initial amount of PVP does not seem to influence membrane rejection as its presence had no effect on the PEG rejection of both pristine and aged membranes.

On the other hand the increase in permeability of the aged membranes was found higher for membranes containing PVP than for the pure PES membrane, which suggests that transformations involving PVP contribute to the observed increase in membrane permeability after ageing. Thus, the increase in the membrane permeability could be due to the oxidation of the PVP itself (and its potential leaking from the membrane that can introduce fragile zones in the overall membrane backbone) and/or an acceleration of the PES degradation due to PVP oxidation by-products.

3.2 PVP degradation

In order to evaluate the PVP degradation due to membrane ageing, the pristine and aged membranes were analyzed by ATR-FTIR spectroscopy. An illustration is provided in figure 4 that shows the spectra obtained for both the pristine and aged membranes (PVP initial amount: 16 %). The major difference between the two spectra is located in the region around 1673 cm^{-1} that can be assigned to the C=O vibration of PVP. A decrease and broadening of the band was observed, which is attributed to PVP degradation (ring opening followed by carboxylic acid formation). Another difference between the two spectra can be observed around 1440 cm^{-1}. This band is ascribed to the C–H vibration from the $CH_2C=O$

group of PVP. The disappearance of this small band after membrane exposure to chlorine confirmed the occurrence of PVP degradation.

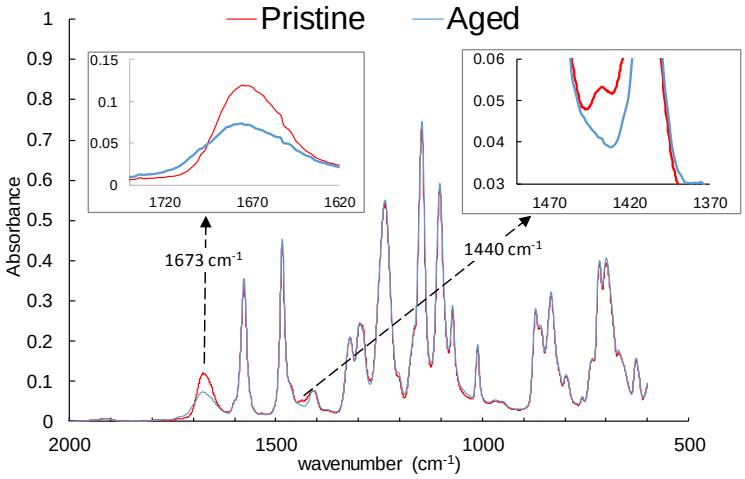

Figure 4: ATR-FTIR spectra of the pristine and fouled membranes (initial amount of PVP: 16 %).

In order to investigate the influence of the PVP amount, the ratio of the bands located at 1673 cm^{-1} and 1235 cm^{-1} (H_{1673}/H_{1235}) was calculated and compared for each membrane sample (figure 5). These bands have been selected as they can be assigned to the C=O vibration of PVP and the C-O-C bond of PES, respectively. Comparing this ratio for the pristine and aged membranes allows to obtain qualitative and quantitative information (provided that a calibration curve can be established) on the relative amount of PVP inside the membrane and on its evolution after membrane ageing [10].

For PVP amounts in the dope solution less than 32 wt % an increase in the H_{1673}/H_{1235} ratio was observed. However, the H_{1673}/H_{1235} ratio was found to level off (H_{1673}/H_{1235} =# 0.3) for higher initial amounts of PVP. This suggests that the PVP-to-PES ratio in the membrane could be different from that in the casting solution (especially for higher PVP amounts), which

could be explained by a release of PVP from the nascent membrane into the non-solvent bath during the phase inversion process.

Furthermore, after ageing a substantial decrease in the H_{1673}/H_{1235} ratio was observed for all membranes regardless of the initial amount of PVP. This confirms that the relative proportion of PVP and PES within the membrane was directly impacted by membrane ageing. The H_{1673}/H_{1235} decrease might be attributed to a partial disappearance (degradation and/or leakage) of the PVP from the membrane surface. PVP degradation could result from a ring opening mechanism and/or succinimide group formation. The formation of succinimide results in a deformation of the C=O band (1670 cm^{-1}) with the appearance of a more or less pronounced shoulder located at slightly higher wavenumbers (around 1700 cm^{-1}) [19]. No shoulder was observed on spectra (figure 4), which suggests that a partial leakage of the PVP from the membrane might have occurred.

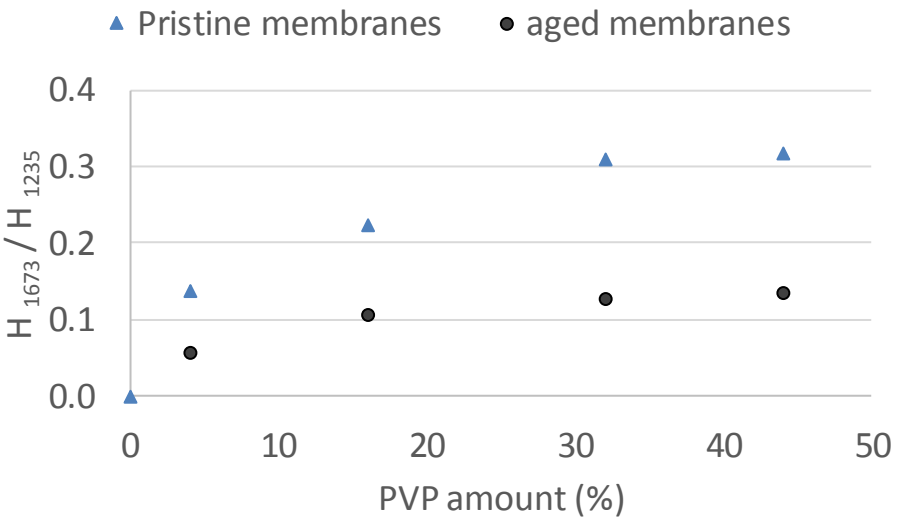

Figure 5: ATR-FTIR characterization (H_{1673}/H_{1235} ratio) of the pristine and aged membranes synthesized with different amounts of PVP (0-44 wt%).

The pristine and aged membranes were further analyzed to map the PVP repartition within the membrane cross-sections. Results obtained with two different samples of membranes synthesized with 32 % of PVP are shown in figure 6. The results obtained for the pristine membrane (top) demonstrate that the PVP repartition was not homogeneous over the membrane cross-section. Indeed a maximum amount of PVP was observed on the membrane top surface (pink/white colors) while the bottom of the membrane contained less PVP (blue color). The PVP repartition over the aged-membrane cross-section is also shown (bottom of figure 6). Even if the pristine membranes were heterogeneous (see differences between samples 1 and 2; top of Figure 6), clear differences can be seen between pristine and aged membranes. After membrane exposure to NaOCl, the maximum amount of PVP was still located at the membrane surface but a significant decrease in the intensity of the PVP signal was observed.

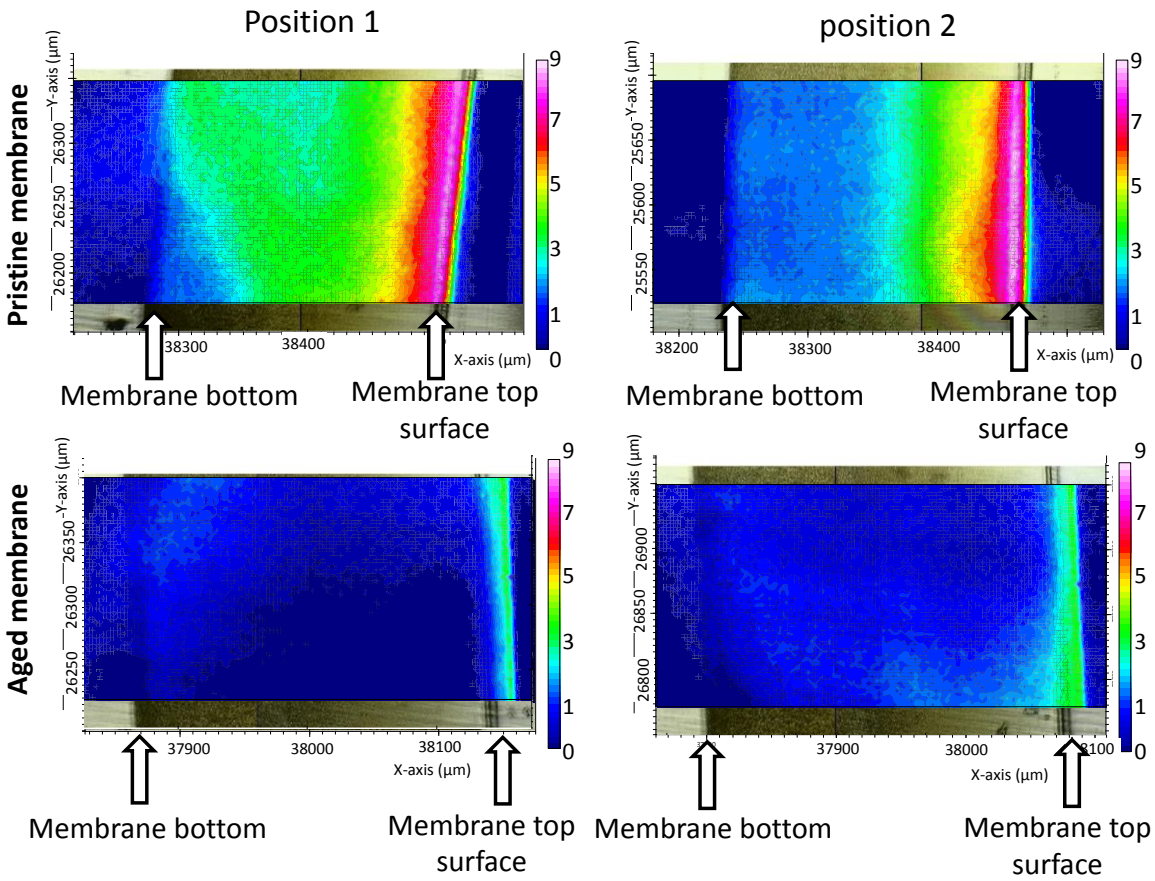

Figure 6: Relative PVP-to-PES ratio mapping over the cross-section of the pristine and aged membranes containing 32 % of PVP (2 samples). The pink color corresponds to the PVP rich zones while the blue color corresponds to the areas containing less PVP. The image in the background is always the light microscopic image of the membrane. (For interpretation of the references to color in this figure legend, the reader is referred to the web version of this article).

This observation confirms that the aged membrane contained less PVP than the pristine membrane, which is in line with results shown in Figure 5.

In order to check that the above observations resulted from exposure to NaOCl and not only to physical wrenching due to the permeate flow through the membrane pure water filtration was performed with pristine membranes for 20 hours. No modification of the H_{1673}/H_{1235} ratio was observed before and after pure water filtration (see supporting information S2), which confirms that NaOCl was responsible for the PVP disappearance (degradation and/or leakage).

3.3 PES oxidation

The membrane surface charge was determined from the streaming current method. For the sake of accuracy electrokinetic measurements were conducted under controlled atmosphere by means of nitrogen gas and the results were interpreted in terms of net charge density (σ_{net}) so as to (i) avoid artifacts caused by carbon dioxide dissolution and (ii) account for the increase in electrical conductivity occurring at low and high pH [13,14,25].

Figure 7 shows the pH dependence of the net charge density for the pristine and aged membranes.

The addition of PVP to PES led to a shift of the membrane isoelectric point (iep) from about 3.7 for the pure PES membrane to about 2.9 for membranes containing PVP. Interestingly, the iep shift was found to be independent of the amount of PVP (in the range 4 – 44 %).

Monitoring the pH dependence of the net charge density revealed the disappearance of the membrane iep after ageing. This phenomenon is the signature of the formation of strong acid groups such as sulfonic acids, as a result of PES-chain scission (see reaction scheme in Figure 8) induced by HClO and HO°. The resulting increase in the number of ionizable groups

onto the membrane surface led to the increase (in absolute value) of the net charge density of the membrane surface after ageing (figure 7).

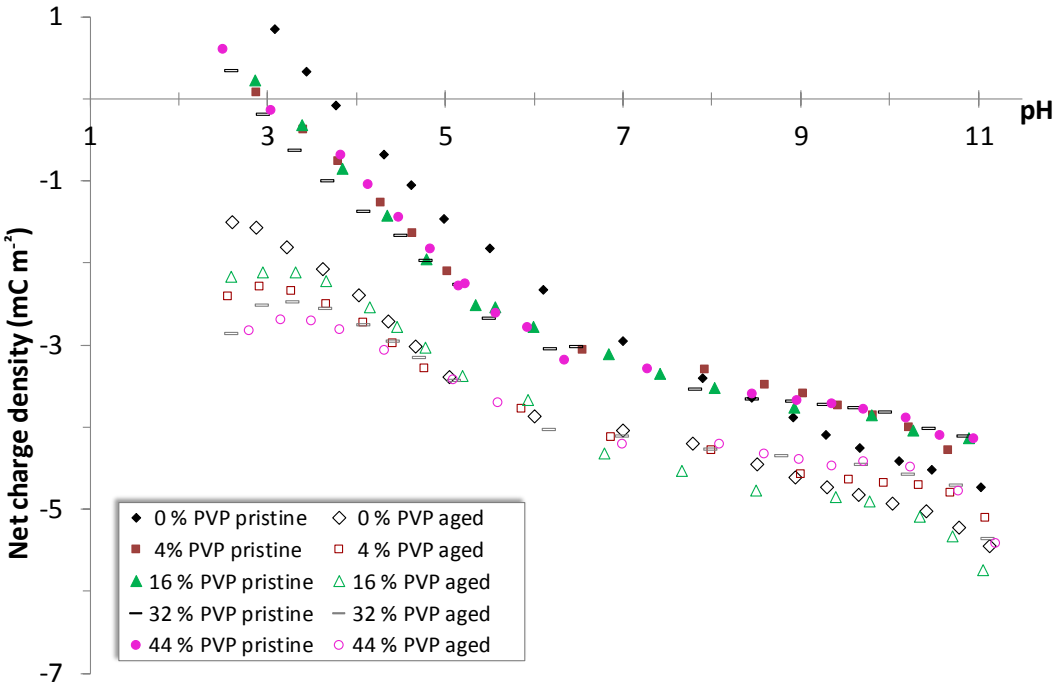

Figure 7: pH dependence of the net charge density of the pristine and aged membranes with different PVP contents (0 to 44 %).

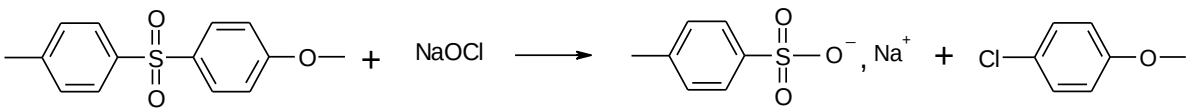

Figure 8: Formation of sulfonic acid groups as a result of PES-chain scission [14].

Interestingly, streaming current measurements showed that PES-chain scissions occurred even with the pure PES membrane. This finding therefore indicates that PVP was not responsible for initiating the PES chain scission mechanism under the present ageing conditions.

Moreover, the electrokinetic curves of aged membranes showed an inflection point at high pH (*ca* 10). This is associated with the ionization of functional groups having very weak acid properties, which is relevant with the formation of phenol groups, likely by radical oxidation of the PES aromatic rings (see PES hydroxylation reaction scheme in figure 9).

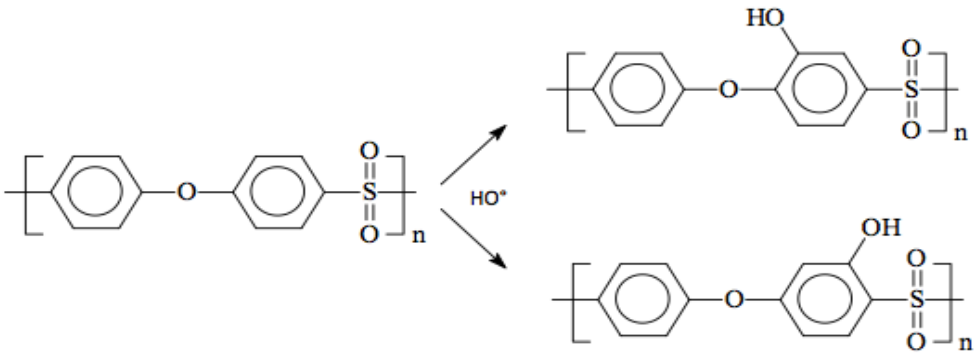

Figure 9: Mechanism of phenol formation through PES radical oxidation [19].

The following procedure was considered in order to analyze data obtained at high pH:

(i) The variation of the experimental net charge density as a function of pH was first fitted by a 6^{th} order polynomial ($r^2 > 0.99$ was obtained for all membranes, see example in the supporting information S3)

(ii) The first derivative of this polynomial ($d\sigma_{net}/dpH$) was determined

(iii) Discrete $d\sigma_{net}/dpH$ values were calculated, focusing on high pH values

This indirect method enabled to more easily differentiate between the behaviors of the different membranes. Indeed, a constant $d\sigma_{net}/dpH$ value reveals a linear variation of σ_{net} with pH while increasing $d\sigma_{net}/dpH$ values (in absolute value) with pH indicate a nonlinear increase in the absolute value of σ_{net}, which can be associated with the ionization of functional groups onto the membrane surface. It should be stressed that ATR-FTIR spectroscopy was not suited here to investigate PES hydroxylation because both sulfonic acid and phenol groups lead to the appearance of a weak band in the same region (about 1030 cm^{-1}).

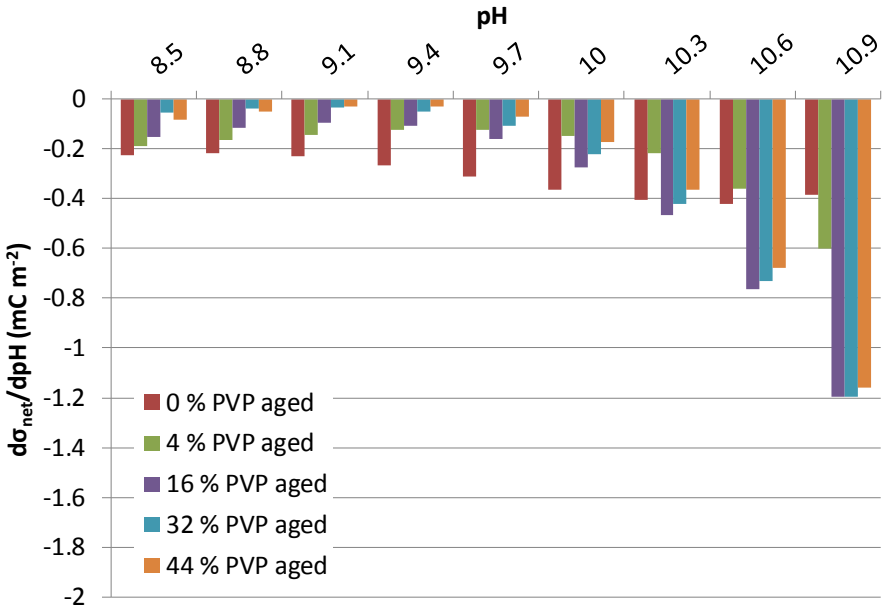

Figure 10: pH dependence of $d\sigma_{net}/dpH$ for the aged membranes with different PVP content (0 to 44 %).

Results obtained for the various aged membranes are depicted in figure 10 which shows that the $d\sigma_{net}/dpH$ values obtained with the aged pure PES membrane were relatively constant with pH, meaning that the variation of σ_{net} against pH was relatively linear for this membrane

460 and thus no PES hydroxylation occurred. On the other hand, for membranes containing PVP
461 an increase in $d\sigma_{net}/dpH$ (in absolute value) with pH was observed for pH > 9, thus indicating
462 PES hydroxylation. This finding shows that the presence of PVP favors the formation of
463 phenol groups onto the PES backbone, which agrees well with Pruhlo et al [19].

464 At high pH the $d\sigma_{net}/dpH$ value is expected to be related to the PES hydroxylation rate.
465 According to figure 10, the PES hydroxylation rate therefore depends the amount of PVP. For
466 instance, at a pH 10.9 $d\sigma_{net}/dpH$ was about -0.35 mC m^{-2} for the pure PES membrane while it
467 was about -0.6 mC m^{-2} for the membrane synthesized with 4 % of PVP and -1.2 mC m^{-2} for
468 the membranes synthesized with higher PVP amounts.

469 In order to confirm the influence of PVP on the PES hydroxylation process, another set of
470 membranes was synthesized using a dope solution containing a lower amount of PES,
471 namely 23 g of PES (instead of 25 g) for 77 g of NMP (instead of 75 g), and PVP-to-PES ratios
472 from 0 to 44 wt %. These membranes were dynamically aged and then characterized by
473 streaming current measurements. As shown in figure S4 of the supporting information the
474 plots of $d\sigma_{net}/dpH$ vs. pH exhibits similar trends as those obtained with the membranes
475 synthesized from a 25 % PES dope solution (figure 10), which confirms that the PES
476 hydroxylation rate was related to the presence and the concentration of PVP in the
477 membrane matrix.

478 As shown previously (see figure 3), the aged membranes exhibited similar PEG rejection
479 performance whatever the PVP content (from 0 to 44 wt %). It can then be concluded that
480 PES hydroxylation has no influence on neutral solute rejection. Moreover, as shown in figure
481 10, the PES hydroxylation rate was lower for the membrane containing 4 % of PVP compared
482 with membranes containing more PVP (16 % - 44 %). However, it has been shown previously

that the permeability of the aged PES/PVP membranes was independent of the PVP amount (see figure 2), which means that PES hydroxylation has no influence on membrane permeability.

3.4 Membrane structure

Information about the membrane structure, before and after exposure to sodium hypochlorite, was obtained by membrane cross-section imaging. Figure 11 shows the cross-section SEM images of the pristine PES membrane as well as the PES/PVP membranes with 4 % and 44 % of PVP. The top images are overview images and show the whole membranes cross-section (the membrane active layer is located on the top of the pictures while the inhomogeneous area below represents the non-woven polypropylene/polyethylene support). The bottom pictures are more detailed pictures of the membranes' top layer.

The membranes containing PVP were rather dense with a top layer of a few tens of micrometers. This could be explained by the high PES content in the casting solution (25 g for 75 g of NMP), thus leading to a solution with high viscosity, which favored the formation of membranes with less macrovoids compared with membranes synthesized from casting solutions containing lower PES concentrations [27,28]. On the other hand, the pure PES membrane exhibited a more asymmetrical structure with the presence of macrovoids of a few micrometers in length. Interestingly, this membrane exhibited a lower permeability than the PES/PVP membranes, which could be explained by the hydrophilic nature of PVP.

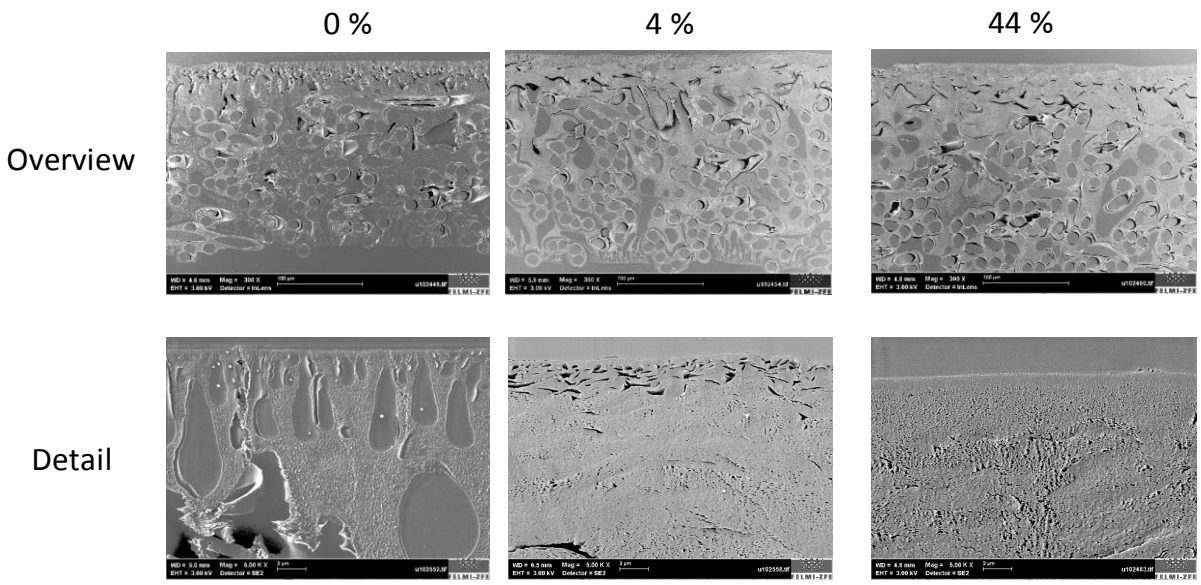

Figure 11: SEM cross-section images of the pristine pure PES membrane, 4 % PVP membrane and 44 % PVP membrane: overview pictures (top) and detailed pictures of the active layer (bottom)

Figure 12 shows the SEM images of the cross-section of the aged membranes (pure PES membrane, PES/PVP membrane with 4 % of PVP and PES/PVP membrane with 44 % of PVP). As for the pristine membranes, both overview and detailed pictures are provided. From these pictures, it clearly appears that the structures of the PES/PVP membranes were impacted by membrane exposure to sodium hypochlorite solution as macrovoids appeared in the membrane structures. The aged membranes exhibited a dense active layer under which a sublayer with cavities of few micrometers was observed. Less pronounced structural differences were observed for the pure PES membrane before and after ageing. These results are in accordance with the permeability data since it was shown that the increase in membrane permeability after ageing was greater for PES/PVP membranes than for the pure PES membrane.

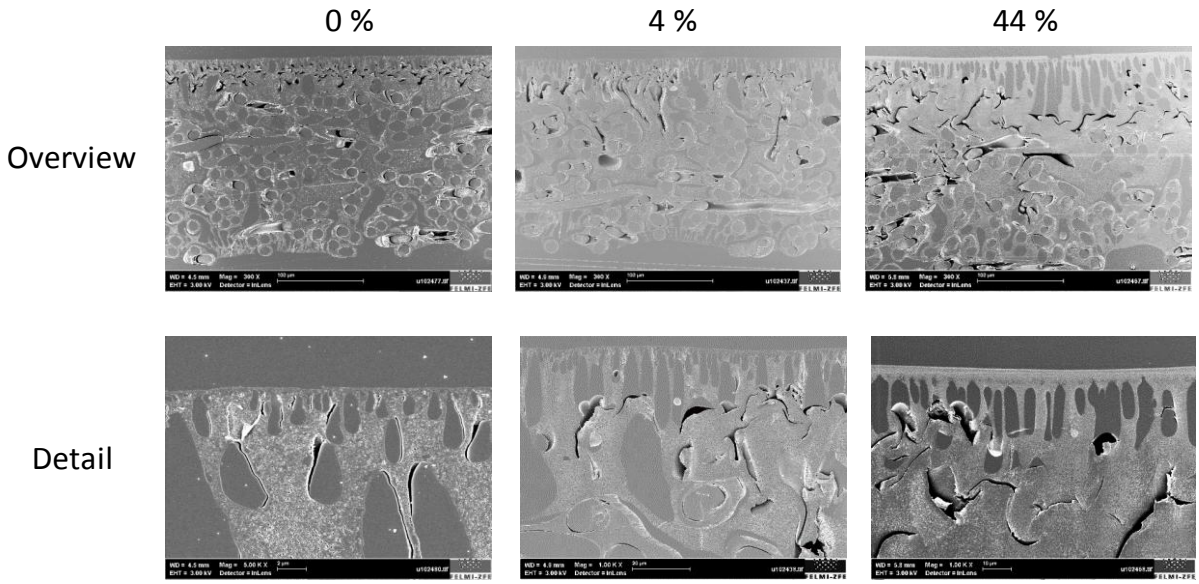

Figure 12: SEM cross-section images of the aged pure PES membrane, 4 % PVP membrane and 44% PVP membrane: overview pictures (top) and detailed pictures of the active layer (bottom)

Conclusion

This work focused on the role of PVP in the degradation mechanisms of PES/PVP membranes exposed to sodium hypochlorite. PES/PVP membranes with PVP-to-PES ratios up to 44 % were synthesized and further chemically aged by 200 ppm TFC hypochlorite solutions at pH 8 under dynamic conditions (filtration over 20 h at room temperature under a TMP of 1 bar).

PVP oxidation, leading to its partial disappearance from the membrane matrix, occurred whatever the membrane composition, thus confirming that PVP is the Achilles' heel of PES/PVP membranes. However, in the tested conditions, PVP leakage seems to have no impact on the membrane retention.

Furthermore, thanks to electrokinetic characterization of both pristine and aged membranes, it was possible to show that PES was also degraded by sodium hypochlorite. PES chain-scissions were observed for all membranes even in the absence of PVP, thus indicating that PVP (or its degradation by-products) is not responsible for the initiation of the PES-chain scission for the present ageing conditions (an impact of PVP on the PES-chain scission kinetics might exist but it was not observed in the present work). On the other hand, it was shown that PES hydroxylation was favored by the presence of PVP. Moreover, exposure of PES/PVP membranes to sodium hypochlorite led to the appearance of macrovoids in the membrane sub-layer.

It was also shown that the membrane permeability increased and the PEG rejection decreased after membrane ageing, whatever the PVP amount (even for the pure PES membrane). It suggests that the PES-chain scission mechanism, that was the only degradation mechanism observed for the pure PES membrane, has an influence on the membrane filtration performance. On the other hand, it was found that PES hydroxylation has no effect on the membrane filtration performance (pure water permeability and PEG rejection).

From the practical point of view, these results underline the necessity to find operating conditions (membrane composition, cleaning-in-place parameters) that enable to avoid PES-chain scissions and additives leaching from the matrix body. Future studies should thus focus on these points rather than on PES hydroxylation mitigation.

Appendix A. Supporting information

Supplementary data associated with this article can be found in the online version.

Acknowledgments

Claudia Mayrhofer and Christian Brandl (Graz Centre of Electron Microscopy) are acknowledged for their help in sample preparation and micro-FTIR-measurements respectively.

References

[1] I.M. Wienk, E.E.B. Meuleman, Z. Borneman, T. van den Boomgaard, C.A. Smolders, Chemical treatment of membranes of a polymer blend: Mechanism of the reaction of hypochlorite with poly(vinyl pyrrolidone), J. Polym. Sci. Part Polym. Chem. 33 (1995) 49–54. doi:10.1002/pola.1995.080330105.

[2] E. Arkhangelsky, D. Kuzmenko, V. Gitis, Impact of chemical cleaning on properties and functioning of polyethersulfone membranes, J. Membr. Sci. 305 (2007) 176–184. doi:10.1016/j.memsci.2007.08.007.

[3] B. Pellegrin, R. Prulho, A. Rivaton, S. Thérias, J.-L. Gardette, E. Gaudichet-Maurin, C. Causserand, Multi-scale analysis of hypochlorite induced PES/PVP ultrafiltration membranes degradation, J. Membr. Sci. 447 (2013) 287–296. doi:10.1016/j.memsci.2013.07.026.

[4] B. Van Der Bruggen, C. Vandecasteele, T. Van Gestel, W. Doyen, R. Leysen, A review of pressure-driven membrane processes in wastewater treatment and drinking water production, Environ. Prog. 22 (2003) 46–56. doi:10.1002/ep.670220116.

[5] J. Marchese, M. Ponce, N.A. Ochoa, P. Prádanos, L. Palacio, A. Hernández, Fouling behaviour of polyethersulfone UF membranes made with different PVP, J. Membr. Sci. 211 (2003) 1–11. doi:10.1016/S0376-7388(02)00260-0.

[6] J. Barzin, S.S. Madaeni, H. Mirzadeh, M. Mehrabzadeh, Effect of polyvinylpyrrolidone on morphology and performance of hemodialysis membranes prepared from polyether sulfone, J. Appl. Polym. Sci. 92 (2004) 3804–3813. doi:10.1002/app.20395.

[7] H. Wang, T. Yu, C. Zhao, Q. Du, Improvement of hydrophilicity and blood compatibility on polyethersulfone membrane by adding polyvinylpyrrolidone, Fibers Polym. 10 (2009) 1–5. doi:10.1007/s12221-009-0001-4.

[8] N. Porcelli, S. Judd, Chemical cleaning of potable water membranes: A review, Sep. Purif. Technol. 71 (2010) 137–143. doi:10.1016/j.seppur.2009.12.007.

[9] V. Puspitasari, A. Granville, P. Le-Clech, V. Chen, Cleaning and ageing effect of sodium hypochlorite on polyvinylidene fluoride (PVDF) membrane, Sep. Purif. Technol. 72 (2010) 301–308. doi:10.1016/j.seppur.2010.03.001.

[10] M. Rabiller-Baudry, A. Bouzin, C. Hallery, J. Girard, C. Leperoux, Evidencing the chemical degradation of a hydrophilised PES ultrafiltration membrane despite protein fouling, Sep. Purif. Technol. 147 (2015) 62–81. doi:10.1016/j.seppur.2015.03.056.

[11] K. Yadav, K.R. Morison, Effects of hypochlorite exposure on flux through polyethersulphone ultrafiltration membranes, Food Bioprod. Process. 88 (2010) 419–424. doi:10.1016/j.fbp.2010.09.005.

[12] B. Pellegrin, F. Mezzari, Y. Hanafi, A. Szymczyk, J.-C. Remigy, C. Causserand, Filtration performance and pore size distribution of hypochlorite aged PES/PVP ultrafiltration membranes, J. Membr. Sci. 474 (2015) 175–186. doi:10.1016/j.memsci.2014.09.028.

[13] Y. Hanafi, A. Szymczyk, M. Rabiller-Baudry, K. Baddari, Degradation of Poly(Ether Sulfone)/Polyvinylpyrrolidone Membranes by Sodium Hypochlorite: Insight from Advanced Electrokinetic Characterizations, Environ. Sci. Technol. 48 (2014) 13419–13426. doi:10.1021/es5027882.

[14] Y. Hanafi, P. Loulergue, S. Ababou-Girard, C. Meriadec, M. Rabiller-Baudry, K. Baddari, A. Szymczyk, Electrokinetic analysis of PES/PVP membranes aged by sodium hypochlorite solutions at different pH, J. Membr. Sci. 501 (2016) 24–32. doi:10.1016/j.memsci.2015.11.041.

[15] C. Causserand, B. Pellegrin, J.-C. Rouch, Effects of sodium hypochlorite exposure mode on PES/PVP ultrafiltration membrane degradation, Water Res. 85 (2015) 316–326. doi:10.1016/j.watres.2015.08.028.

[16] E. Arkhangelsky, D. Kuzmenko, N.V. Gitis, M. Vinogradov, S. Kuiry, V. Gitis, Hypochlorite Cleaning Causes Degradation of Polymer Membranes, Tribol. Lett. 28 (2007) 109–116. doi:10.1007/s11249-007-9253-6.

[17] G. Holst, The Chemistry of Bleaching and Oxidizing Agents., Chem. Rev. 54 (1954) 169–194. doi:10.1021/cr60167a005.

[18] K. Fukatsu, S. Kokot, Degradation of poly(ethylene oxide) by electro-generated active species in aqueous halide medium, Polym. Degrad. Stab. 72 (2001) 353–359. doi:10.1016/S0141-3910(01)00037-4.

[19] R. Prulho, S. Therias, A. Rivaton, J.-L. Gardette, Ageing of polyethersulfone/polyvinylpyrrolidone blends in contact with bleach water, Polym. Degrad. Stab. 98 (2013) 1164–1172. doi:10.1016/j.polymdegradstab.2013.03.011.

[20] M. Nachtnebel, H. Fitzek, C. Mayrhofer, B. Chernev, P. Pölt, Spatial localization of membrane degradation by in situ wetting and drying of membranes in the scanning electron microscope, J. Membr. Sci. 503 (2016) 81–89. doi:10.1016/j.memsci.2015.12.046.

627 [21] L. Bégoin, M. Rabiller-Baudry, B. Chaufer, M.-C. Hautbois, T. Doneva, Ageing of PES
628 industrial spiral-wound membranes in acid whey ultrafiltration, Desalination. 192
629 (2006) 25–39. doi:10.1016/j.desal.2005.10.009.
630 [22] K. Yadav, K. Morison, M.P. Staiger, Effects of hypochlorite treatment on the surface
631 morphology and mechanical properties of polyethersulfone ultrafiltration membranes,
632 Polym. Degrad. Stab. 94 (2009) 1955–1961.
633 doi:10.1016/j.polymdegradstab.2009.07.027.
634 [23] D. Delaunay, Nettoyage éco-efficace de membranes planes et spirales d'ultrafiltration
635 de lait écrémé : approches physico-chimiques et hydrodynamiques concertées, Rennes
636 1, 2007. http://www.theses.fr/2007REN1S094 (accessed September 22, 2016).
637 [24] M. Rabiller-Baudry, C. Lepéroux, D. Delaunay, H. Diallo, L. Paquin, On the use of
638 microwaves to accelerate ageing of an ultrafiltration PES membrane by sodium
639 hypochlorite to obtain similar ageing state to that obtained for membranes working at
640 industrial scale, Filtration. 14 (2014) 38–48.
641 [25] E. Idil Mouhoumed, A. Szymczyk, A. Schäfer, L. Paugam, Y.H. La, Physico-chemical
642 characterization of polyamide NF/RO membranes: Insight from streaming current
643 measurements, J. Membr. Sci. 461 (2014) 130–138. doi:10.1016/j.memsci.2014.03.025.
644 [26] A.F. Ismail, A.R. Hassan, Effect of additive contents on the performances and structural
645 properties of asymmetric polyethersulfone (PES) nanofiltration membranes, Sep. Purif.
646 Technol. 55 (2007) 98–109. doi:10.1016/j.seppur.2006.11.002.
647 [27] K. Boussu, C. Vandecasteele, B. Van der Bruggen, Study of the characteristics and the
648 performance of self-made nanoporous polyethersulfone membranes, Polymer. 47
649 (2006) 3464–3476. doi:10.1016/j.polymer.2006.03.048.

[28] G.R. Guillen, Y. Pan, M. Li, E.M.V. Hoek, Preparation and Characterization of Membranes Formed by Nonsolvent Induced Phase Separation: A Review, Ind. Eng. Chem. Res. 50 (2011) 3798–3817. doi:10.1021/ie101928r.

671 **Supporting information**

672

673 Yamina Kourde-Hanafi[1,2], Patrick Loulergue[1*], Jean-Luc Audic[1], Murielle Rabiller-Baudry[1],

674 Manfred Nachtnebel[3], Peter Pölt[3,4], Kamel Baddari[2], Bart Van der Bruggen[5], Anthony

675 Szymczyk[1]

676 [1]Université de Rennes 1, Université Bretagne-Loire, Institut des Sciences Chimiques de

677 Rennes (UMR CNRS 6226), 263 Avenue du Général Leclerc, CS 74205, 35042 Rennes, France

678 [2]Unité de Recherche Matériaux Procédés et Environnement, Université M'hamed Bougara,

679 Boumerdes, Algeria

680 [3]Institute for Electron Microscopy and Nanoanalysis, NAWI Graz, Graz University of

681 Technology, Steyrerg. 17, 8010 Graz, Austria

682 [4]Graz Centre for Electron Microscopy, Steyrerg. 17, 8010 Graz, Austria

683 [5]Department of Chemical Engineering, KU Leuven, Celestijnenlaan 200F, B-3001 Heverlee,

684 Belgium

685 * corresponding author : patrick.loulergue.1@univ-rennes1.fr

686

687

688

689

690

691

692

Figure S1. Pure water flux through pure PES aged membranes (J_w) against transmembrane pressure (TMP) (the slope represents the membrane permeability according to Darcy's Law).

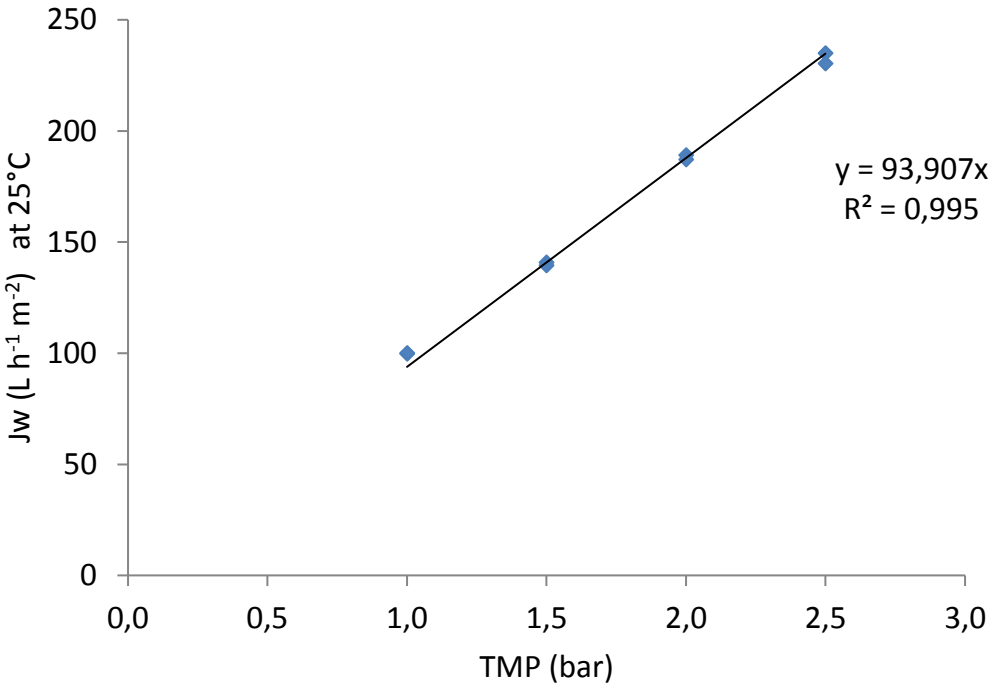

Figure S2. ATR-FTIR characterization (H_{1673}/H_{1235} ratio) of the pristine membrane before and after pure water filtration (20 h, 1 bar)

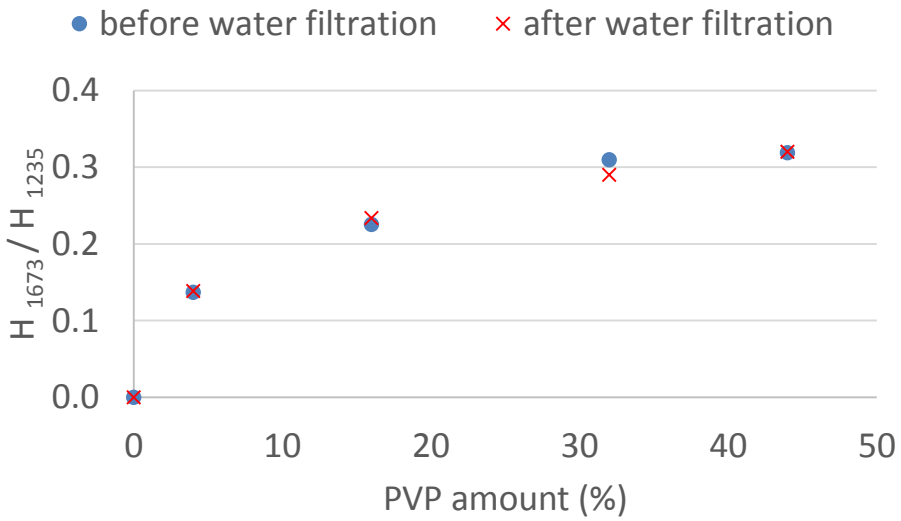

Figure S3. Example of modelling of pH dependence of the net charge density of the aged membrane (PVP-to-PES ratio: 16 %) by a 6th order polynomial.

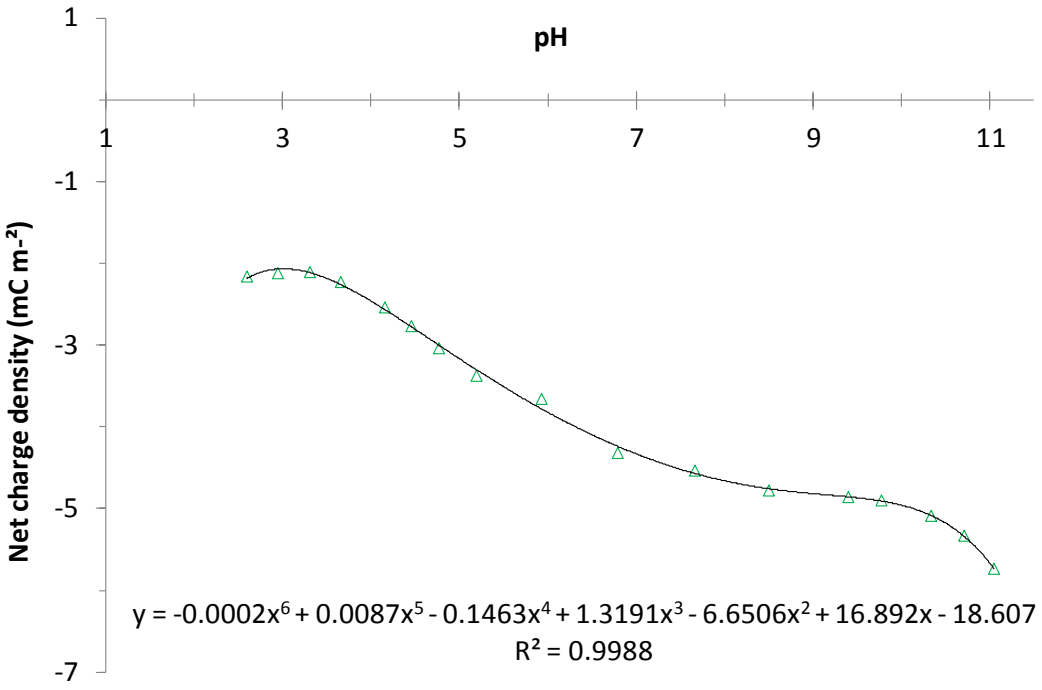

730 **Figure S4. pH dependence of $d\sigma_{net}/dpH$ for the aged membranes with a PES mass of 23 g**

731 **and a NMP mass of 77 g and different PVP content (0 to 44 % PVP-to-PES ratio)**

732

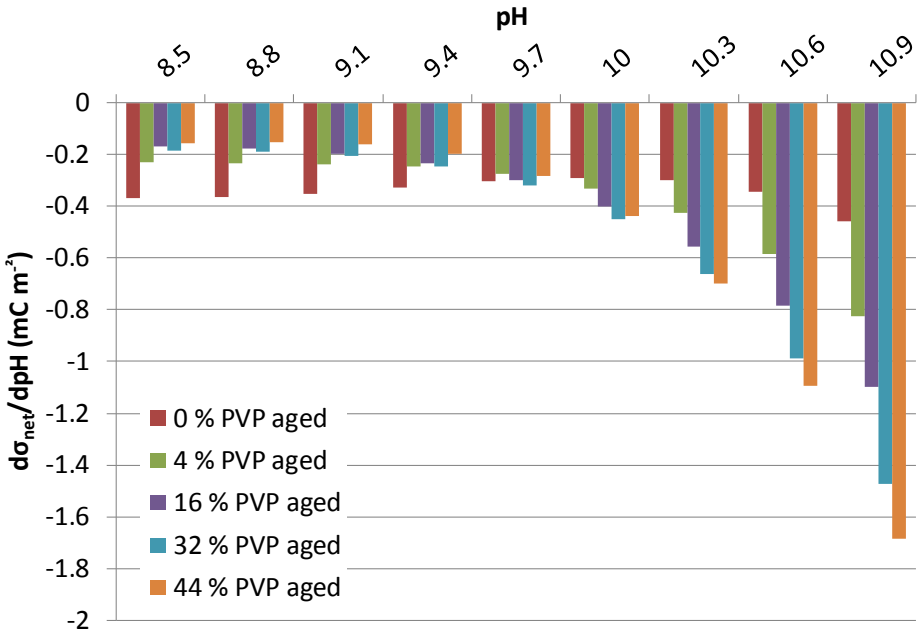

733